CHEMBIOCHEM

DOI: 10.1002/cbic.201000639

Spacer Effects on in vivo Properties of DOTA-Conjugated Dimeric [Tyr3]Octreotate Peptides Synthesized by a "Cu^{I}-Click" and "Sulfo-Click" Ligation Method

Cheng-Bin Yim,[a, b] Berend van der Wildt,[a] Ingrid Dijkgraaf,[b] Lieke Joosten,[b] Annemarie Eek,[b] Cees Versluis,[c] Dirk T. S. Rijkers,[a] Otto C. Boerman,[b] and Rob M. J. Liskamp*[a]

We report on the SSTR2-binding properties of a series of four dimeric [Tyr3]octreotate analogues with different spacer lengths (nine, 19, 41, and 57 atoms) between the peptides. Two analogues (9 and 57 atoms) were selected as precursors for the design, synthesis, and biological evaluation of DOTA-conjugated dimeric [Tyr3]octreotate analogues for tumor targeting. These compounds were synthesized by using a two-stage click ligation procedure: a Cu^{I}-catalyzed 1,3-dipolar cycloaddition ("copper-click" reaction) and a thio acid/sulfonyl azide amidation ("sulfo-click" reaction). The IC_{50} values of these DOTA-conjugated [Tyr3]octreotate analogues were comparable, and internalization studies showed that the nine-atom ^{111}In-DOTA-labeled [Tyr3]octreotate dimer had rapid and high receptor binding. Biodistribution studies with BALB/c nude mice bearing subcutaneous AR42J tumors showed that the ^{111}In-labeled [Tyr3]octreotate dimer (nine atoms) had a high tumor uptake at 1 h p.i. ($38.8 \pm 8.3\%$ ID g^{-1}), and excellent tumor retention at 4 h p.i. ($40.9 \pm 2.5\%$ ID g^{-1}). However, the introduction of the extended hydrophilic 57 atoms spacer led to rapid clearance from the circulation; this limited tumor accumulation of the radiotracer ($21.4 \pm 4.9\%$ ID g^{-1} at 1 h p.i.). These findings provide important insight on dimerization and spacer effects on the in vivo properties of DOTA-conjugated [Tyr3]octreotate dimers.

Introduction

Somatostatin is a regulatory hormone with diverse physiological inhibitory actions on various gastrointestinal functions, including the secretion of gastrin, insulin, glucagon, and growth hormone.[1] These biological effects are mediated by a family of five specific G protein-coupled cell-surface receptors, the somatostatin receptors (SSTRs).[2] As some of these receptors are overexpressed, in particular subtype 2 (SSTR2) on most neuroendocrine tumor cells, native somatostatin has been viewed as an ideal candidate for the treatment of these tumors. However, its rapid proteolytic degradation (plasma half-life < 3 min) has limited its clinical usefulness. Structure–activity studies have been carried out with a variety of synthetic analogues that have enhanced stability towards enzymatic degradation, and different affinities for each receptor subtype.[3] Clinical studies have shown that [Tyr3]octreotate, an octapeptide analogue of somatostatin, is effective in the treatment of endocrine pancreatic tumors.[4]

There is growing interest in the development of multimeric peptide and carbohydrate conjugates, because they have enhanced receptor affinity when compared to their corresponding monomeric analogues.[5] For example, it has been demonstrated that radiolabeled (^{68}Ga, ^{99m}Tc, and ^{111}In) dimeric, cyclic arginine–glycine–aspartic acid (RGD) peptides have higher tumor uptake and longer tumor retention than their corresponding monomeric counterparts.[6,7] In vitro assays and in vivo studies have shown that several cyclic RGD-peptide dimers bind bivalently to their $\alpha_v\beta_3$ receptors because of adequate spacing between two RGD motifs.[7] Presently, there are no reports that identify whether dimeric [Tyr3]octreotate binds in a similar fashion. This is particularly relevant because recent studies have established that some somatostatin receptors associate as homo- and heterodimers.[8] However, the design of bivalent ligands (where the spacing of two tailored targeting vectors is suited for simultaneous binding to adjacent receptor sites) is for the most part a highly empirical endeavor. The main objective of this study was to determine the SSTR2-binding properties of dimeric [Tyr3]octreotate analogues, and to

[a] C.-B. Yim, B. van der Wildt, Dr. D. T. S. Rijkers, Prof. Dr. R. M. J. Liskamp
Division of Medicinal Chemistry and Chemical Biology
Utrecht Institute for Pharmaceutical Sciences
Department of Pharmaceutical Sciences, Utrecht University
P.O. Box 80082, 3508 TB Utrecht (The Netherlands)
Fax: (+31) 30-2536655
E-mail: r.m.j.liskamp@uu.nl

[b] C.-B. Yim, Dr. I. Dijkgraaf, L. Joosten, A. Eek, Prof. Dr. O. C. Boerman
Department of Nuclear Medicine, Radboud University Nijmegen Medical Centre
P.O. Box 9101, 6500 HB Nijmegen (The Netherlands)

[c] C. Versluis
Biomolecular Mass Spectrometry and Proteomics Group
Bijvoet Center for Biomolecular Research and
Utrecht Institute for Pharmaceutical Sciences
Department of Pharmaceutical Sciences, Utrecht University
P.O. Box 80082, 3508 TB Utrecht (The Netherlands)

Supporting information for this article is available on the WWW under http://dx.doi.org/10.1002/cbic.201000639.

assess the effects of different spacers between the two targeting ligands on the in vitro and in vivo characteristics.

Results and Discussion

Rationale for the design

A series of dimeric [Tyr3]octreotate peptides, with different spacers, has been synthesized and evaluated for their receptor binding. These conjugates were prepared by Cu^{I}-catalyzed 1,3-dipolar cycloaddition[9] between peptidyl azides and dimeric alkynes. The investigated spacer lengths were nine, 19, 41, and 57 atomic units, as measured between the two alkyne moieties. As an example, Scheme 1 depicts the dimeric alkyne building block with the shortest (nine-atom) spacer. The IC_{50} values of the dimeric [Tyr3]octreotate derivatives **7**–**11**, obtained from competitive binding assays with AR42J tumor cells, were in the low-nanomolar region.

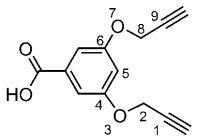

Scheme 1. Molecular structure of the dimeric alkyne building block. Numbers indicate the atoms involved in the spacer.

The dimer with the longest spacer (57 atoms) **11**, which exerted the highest receptor affinity, and the dimer with the shortest spacer (nine atoms) **7** were selected as candidates for DOTA (1,4,7,10-tetraazacyclododecane-1,4,7,10-tetraacetic acid)-conjugation, radiolabeling, and subsequent in vivo evaluation. These DOTA-conjugated dimeric [Tyr3]octreotate derivatives were synthesized by a combination of Cu^{I}-catalyzed 1,3-dipolar cycloaddition and thio acid/sulfonyl azide amidation,[10,11] which have been denoted as "copper-click" and "sulfo-click", respectively. This two-stage click-ligation method has been shown to be very useful for the metal-free and convenient introduction of a metal chelator, like DOTA, in the design of multimeric peptide conjugates for in vivo research applications.[12] A strategy based on sequential click reactions could serve as a powerful process for incorporating virtually any peptide sequence, without interference from other functional groups of the peptide. This ligation procedure avoids the use of protecting groups, and enables versatile conjugation with unprotected peptides. Herein, we describe the application of this two-stage click approach in the design, synthesis, and in vivo characterization of DOTA-conjugated dimeric [Tyr3]octreotate analogues. Biodistribution studies with ^{111}In-labeled compounds were evaluated in a BALB/c nude mouse model with subcutaneous AR42J pancreatic tumors.

Synthesis

Syntheses of [Ahx0,Tyr3]octreotate and dimeric alkynes: The synthesis of the [Tyr3]octreotate analogue with an N-terminal 6-azidohexanoyl (Ahx) linker on solid phase, and its oxidation towards [Ahx0,Tyr3]octreotate **1** is depicted in Scheme 2. This peptide required a C-terminal acid functionality; this was achieved by using the hydroxymethyl-based Wang (HMP) resin. The loading of the first amino acid, Fmoc-Thr(*t*Bu)-OH, was performed by using the esterification approach described by Sieber.[13] The synthesis of the linear peptide followed established Fmoc/*t*Bu chemistry protocols.[14] To enable "copper-click" chemistry, an azide functionality was introduced at the N terminus by HBTU-coupling with 6-azidohexanoic acid. After cleavage from the resin, cyclization of the linear peptide was achieved by DMSO-mediated oxidation of the cysteine thiols.[15] The cyclic [Ahx0,Tyr3]octreotate **1** was obtained in an overall yield of 24%, after preparative HPLC, and identified by mass spectrometry.

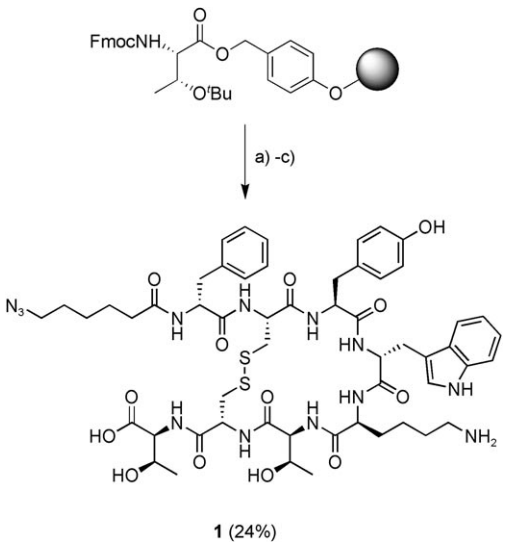

1 (24%)

Scheme 2. Synthesis of [Ahx0,Tyr3]octreotate **1** (Ahx-D-Phe-*cyclo*(Cys-Tyr-D-Trp-Lys-Thr-Cys)-Thr-OH). a) SPPS (HBTU/HOBt/DiPEA); b) TFA/TiPS/H_2O; c) 10% DMSO, H_2O/CH_3CN, pH 8.

We have reported the convergent synthesis of amino acid based dendrimers with peripheral propargyl groups to enable the "copper-click" reaction with peptide-derived azides.[16] This flexible synthetic strategy, based on the dihydroxybenzoic acid moiety, can be easily modified with a variety of branching units, rigidities, cavity sizes, and tunable surface functionalities.[17] Benzoic acid-based monomeric alkyne **2** and dimeric alkynes **3**–**6** (Scheme 3) were prepared following a procedure which was previously described.[18] In addition, to enable the "sulfo-click" reaction with the DOTA metal chelator, a thio acid functionality was introduced. This thio acid moiety can be readily prepared from a 2,4,6-trimethoxybenzyl (TMOB) thio ester precursor, as previously reported.[12] Hence, a selection of mono- and dimeric alkynes **2b**, **3b** and **6b** with TMOB-protected thio acids was synthesized from their corresponding carboxylic acids **2a**, **3a** and **6a**, respectively, as depicted in Scheme 3.

Conjugation of [Ahx0,Tyr3]octreotate to mono- and dimeric alkynes by the "copper-click" reaction procedure: The synthesis route towards the monomeric [Tyr3]octreotate analogue **7** and dimeric [Tyr3]octreotate conjugates **8**–**11** is outlined in Scheme 4. Following general procedures for microwave-assisted "copper-click" chemistry,[12,16,18b,c] azide **1** was reacted with acetylenes **2a**–**6a** in the presence of $CuSO_4$/Na ascorbate in THF/H_2O (1:1, *v*/*v*) under microwave irradiation at 100 °C. HPLC

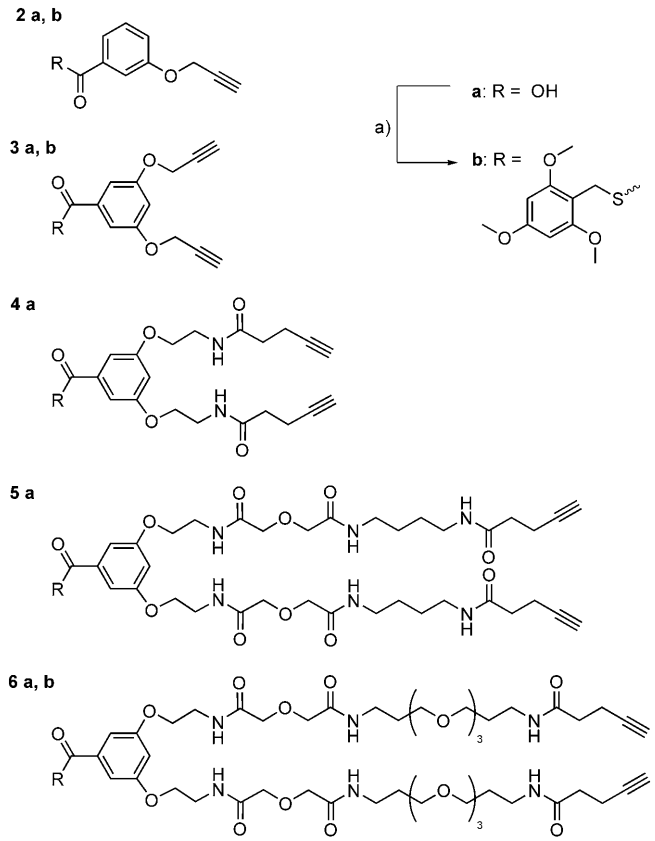

Scheme 3. Dihydroxyenzoic acid-based mono- and dimeric alkynes **2a**–**6a**, and synthesis of TMOB-protected mono- and dimeric thio esters **2b**, **3b**, and **6b** from their carboxcylic acids **2a**, **3a**, and **6a**. a) TMOB-thiol, EDCI, DMAP, DMF, 16 h, RT; yields: **2b** (27%), **3b** (59%), **6b** (58%).

analysis showed complete conversion within 5 min. Optimization studies showed that 0.5 equivalent $CuSO_4$ per alkyne moiety, accompanied by 2.5 equivalent Na ascorbate, gave the best results for the examined click reactions. After semi-preparative HPLC, **7**–**11** were obtained in acceptable to very good yields (33–90%). The identities of the cycloadducts **7**–**11** were confirmed by mass spectrometry. These compounds were not contaminated with any copper species.

Synthesis of mono- and dimeric DOTA-conjugated [Tyr3]octreotate conjugates by the two-stage click ligation method: The preparation of DOTA-conjugated peptide conjugates **16**–**18** by using a combination of "copper-click" chemistry and the "sulfo-click" procedure is shown in Schemes 5 and 6. Analogous to the synthesis of peptide triazoles **7**–**11**, the "copper-click" reaction between azide **1** and alkynes **2b**, **3b** or **6b** was performed in the presence of 0.5 equivalent $CuSO_4$ per alkyne functionality. Under optimized conditions these reactions were allowed to proceed for 16 h at room temperature. After semi-preparative HPLC, triazoles **12**–**14** were isolated in 31–66% yields (Scheme 5). Under these conditions, triazoles **12**–**14** were found to be stable against hydrolysis. These protected thio esters were treated with trifluoroacetic acid/triisopropylsilane (TFA/T*i*PS) to give the free thio acids that were used directly in the subsequent thio acid/sulfonyl azide amidation ("sulfo-click") with DOTA derivative **15** (Scheme 6).[12] This coupling was allowed to run for 1 h at room temperature, and subsequent treatment with TFA/T*i*PS/H_2O removed the *t*Bu groups of DOTA. After purification by HPLC (twice), the N-acylsulfonamides **16**, **17**, and **18** were obtained in overall yields of 43, 22, and 12%, respectively. These DOTA-conjugated [Tyr3]-octreotate conjugates were characterized by a nano-ESI LC-MS system. As an example, Figure 1 shows the high-resolution

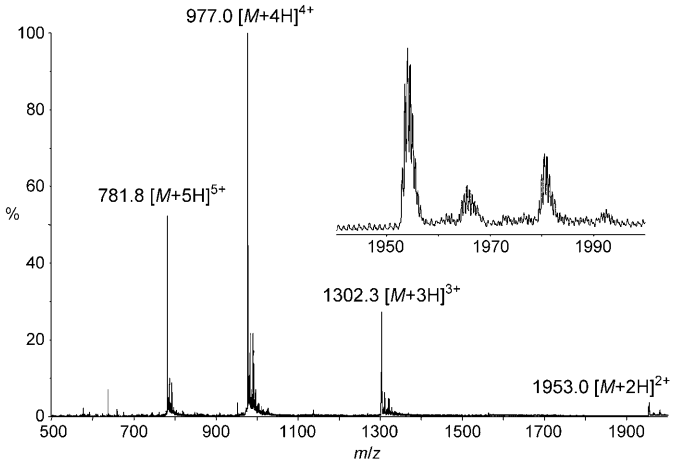

Figure 1. High-resolution ESI-MS mass spectrum of DOTA-conjugated dimeric [Tyr3]octreotate *N*-acylsulfonamide **18**: *m/z* observed, 3903.968; calculated, 3903.700 (monoisotopic).

mass spectrum of DOTA-conjugated dimeric [Tyr3]octreotate analogue **18**. We also tried a "sulfo-click" ligation in which the DOTA moiety was *un*protected; however, the isolated yield of this reaction was not improved. Moreover, to avoid any premature complexation of metal atoms by the unprotected DOTA moiety, we preferred a *t*Bu-protected DOTA moiety during the whole synthesis of the molecular constructs.

To summarize, the four dimeric [Tyr3]octreotate analogues **8**–**11** (with spacers ranging from 9 to 57 atoms) were successfully synthesized using the "copper-click" method between peptidyl azides and alkyne-hydroxy benzoic acid derivatives. The receptor affinities of these dimers were determined by using an in vitro binding assay, and compared to their monomeric counterpart **7**. For subsequent biological characterization, a selection of three DOTA-conjugated [Tyr3]octreotate analogues (**16**–**18**) were prepared by a combination of "copper-click" and "sulfo-click" chemistry. In addition to their in vitro characterization, these compounds were also evaluated for their tumor targeting and pharmacokinetic profiles in an in vivo tumor model.

Receptor binding studies

Binding affinities for the somatostatin receptor of the dimeric [Tyr3]octreotate conjugates **8**–**11**, were determined by using a competitive binding assay on AR42J tumor cells, by using [^{111}In-DOTA0,Tyr3]octreotate as a radiotracer. The IC_{50} values were calculated from fitted sigmoidal displacement curves as depicted in Figure 2 A, and summarized in Table 1. For compar-

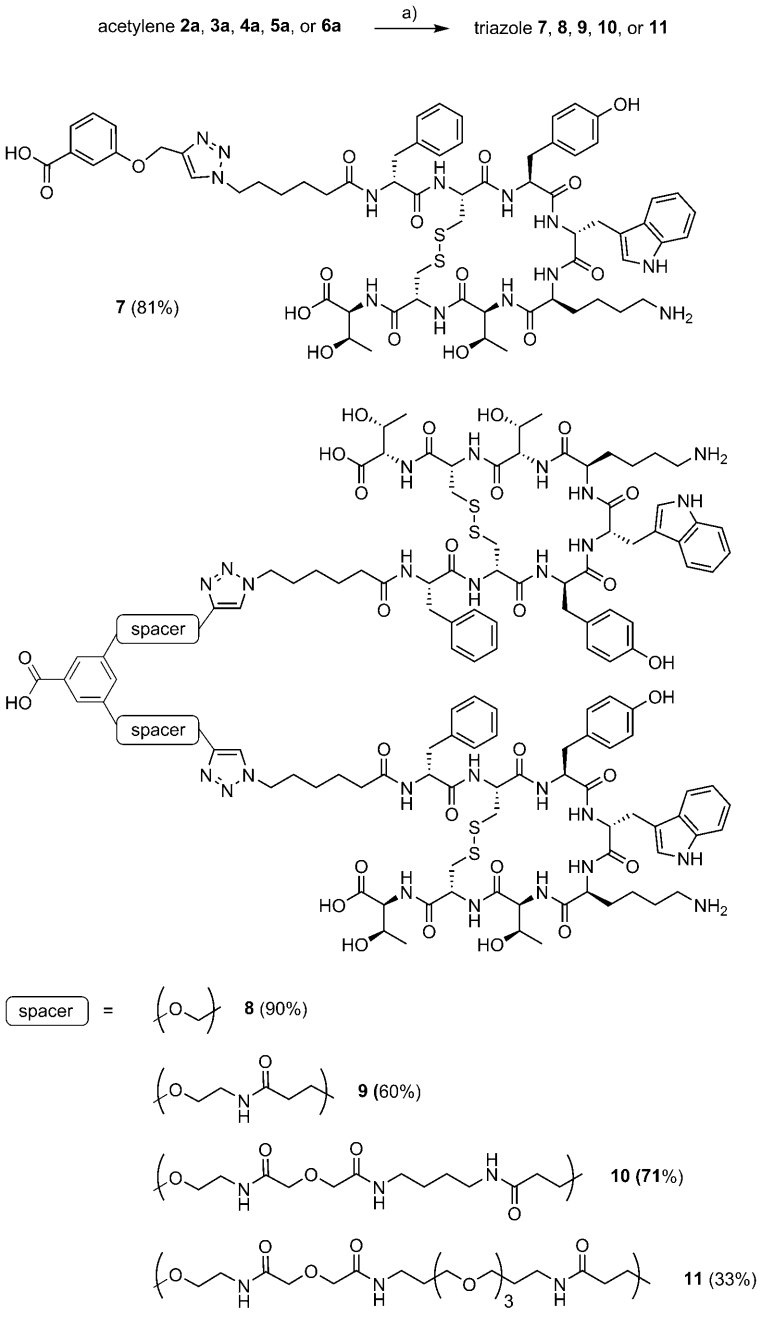

Scheme 4. Synthesis of mono- and dimeric [Tyr3]octreotate triazoles **7**–**11**. a) Azide **1** and $CuSO_4$/Na ascorbate, THF/H_2O, microwave (100 °C), 5 min.

ison, the [Tyr3]octreotate conjugate **7** was also included as one of the competing ligands in the same in vitro assay. All the synthesized compounds showed high receptor binding for the AR42J cell line, as is apparent from the low IC_{50} values: between 1 and 5 nM. Remarkably, the incorporation of different spacers, ranging from 9 to 57 atoms in length, between the two [Tyr3]octreotate motifs resulted in only minor changes to in vitro receptor affinity.

However, dimeric compound **11** had the highest affinity. Therefore, dimeric [Tyr3]octreotate conjugate **11** with the longest spacer (57 atoms), and dimer **8** containing the shortest spacer (nine atoms) were selected as precursors for further in vitro *and* in vivo evaluation, to assess spacer effects on pharmacokinetic properties. Therefore, DOTA-conjugated derivatives **17** and **18**, synthesized by the two-stage click method (vide supra), were tested for their binding properties in a competitive binding assay (Figure 2B). As a reference, DOTA-conjugated monomeric [Tyr3]octreotate analogue **16** was also includeed. The IC_{50} values of these DOTA-containing compounds, labeled with ^{nat}In, are reported in Table 1. With IC_{50} values around 1 nM, the ^{nat}In-DOTA-labeled [Tyr3]octreotate monomer **16**, and dimers **17** and **18** exerted comparable receptor binding. The incorporation of ^{nat}In-DOTA, as in **16**–**18**, led to an overall increase in receptor affinity compared to [Tyr3]octreotate dimers **8**–**11** without the DOTA metal chelator; this was advantageous for the current study.

Lipophilicity studies

The log*D* values of ^{111}In-labeled DOTA-conjugated mono- and dimeric [Tyr3]octreotate sulfonamides **16**, **17**, and **18** were -2.79 ± 0.05, -2.04 ± 0.05 and -1.89 ± 0.13, respectively, and were obtained from n-octanol/saline partition coefficient measurements. Compared to [^{111}In-DOTA0,Tyr3]octreotate ($\log D = -3.63 \pm 0.06$), ^{111}In-labeled compound **16** was slightly more lipophilic (factor: 7×), which may be attributed to the synthetic core moiety (benzoyl core, sulfonamide, triazole, and spacer).

Serum stability studies

To determine the in vitro stability, [Tyr3]octreotate analogues were incubated in human serum, and analyzed at several time intervals. After incubation in human serum at 37 °C for 24 h, ^{111}In-labeled compounds **16**, **17**, and **18** remained intact, as inferred from RP-HPLC. The retention times were 16.2, 17.1, and 16.5 min for **16**, **17**, and **18**, respectively. Fortunately, these ^{111}In-labeled compounds showed high stability: >99% intact

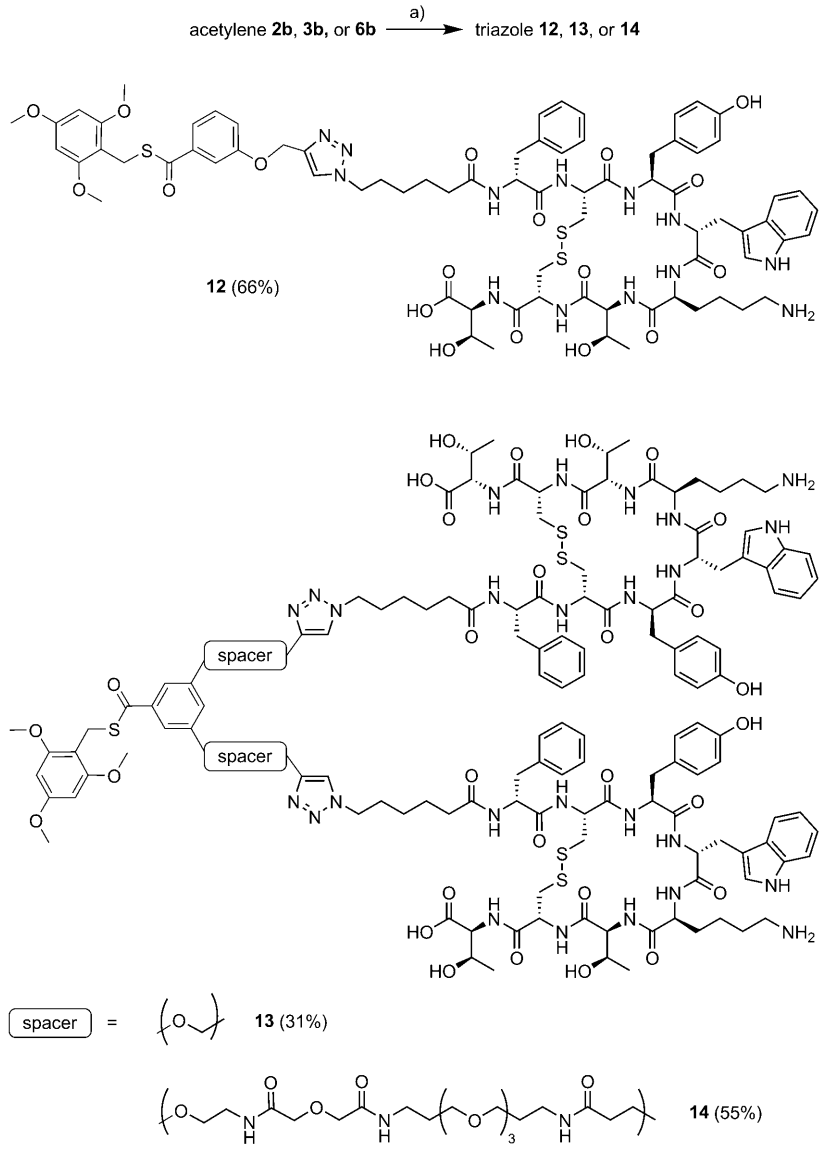

Scheme 5. Synthesis of mono- and dimeric [Tyr3]octreotate triazoles **12**–**14** by the "copper-click" method. a) azide **1**, $CuSO_4$/Na ascorbate, THF/H_2O, 24 h, RT.

Table 1. IC_{50} values for monomeric and dimeric [Tyr3]octreotate analogues **7**–**11** and for ^{nat}In-labeled monomeric and dimeric [Tyr3]octreotate DOTA-conjugated analogues **16**–**18**.[a]

Ligand	Monomer/dimer	IC_{50} [nM]	95% CI[b] [nM]
Non-DOTA			
7	monomer	1.8	1.6–2.0
8	dimer	3.4	3.0–3.9
9	dimer	4.6	3.6–5.8
10	dimer	3.3	2.9–3.8
11	dimer	2.1	1.7–2.7
[^{nat}In]DOTA			
16	monomer	0.7	0.6–0.9
17	dimer	1.0	0.8–1.2
18	dimer	1.0	0.9–1.2

[a] Values were determined by a competitive binding assay with AR42J tumor cells, using [^{111}In-DOTA0,Tyr3]octreotate as a radiotracer. ($n=2$ for each data point). [b] Confidence interval.

peptide, even after 48 h incubation in human serum. These data indicated that the synthetic compounds, with both sulfonamide and triazole linkers, are highly stable in human serum.

Internalization kinetics

Figure 3 A and B shows the receptor binding and internalization rates, respectively, of ^{111}In-labeled **16**–**18** after incubation at 37 °C with AR42J rat pancreatic tumor cells. These radiolabeled [Tyr3]octreotate analogues showed specific and time-dependent cellular uptake. ^{111}In-labeled **16** and **18** exerted a progressive increase in receptor binding, while ^{111}In-labeled **17** had a rapid and high membrane-bound uptake. At 1 h, the membrane-bound activity of ^{111}In-labeled **17** (14.0 ± 0.4%) was twice as high as **16** (6.0 ± 0.1%) or **18** (7.4 ± 0.7%), and remained high after 2 and 4 h of incubation. As shown in Figure 3 B, ^{111}In-labeled **16** had the highest internalization rate (16.7 ± 0.4% at 30 min and 45.7 ± 3.2% at 4 h), followed by **17** (14.7 ± 0.4% at 30 min and 40.1 ± 1.3% at 4 h) and **18** (9.4 ± 0.2% at 30 min and 32.4 ± 3.1% at 4 h).

Biodistribution study

The in vivo tumor targeting of ^{111}In-labeled **16**–**18** was investigated in BALB/c nude mice with subcutaneous SSTR2-expressing AR42J tumors. The organ distribution of ^{111}In-labeled **16**, **17**, and **18** after 1, 4, and 24 h post-injection (p.i.) are summarized in Figure 4 and Table 2. ^{111}In-labeled **16** (Figure 4 A) had a rapid and high tumor uptake (35.99 ± 6.89% ID g^{-1} at 1 h p.i.); this could be blocked by co-injection of an excess of octreotide, which indicates that tumor accumulation was a receptor-mediated process. ^{111}In-labeled [DOTA0, Tyr3]octreotate, the reference compound (Figure S11, and Table S1 in the Supporting Information), had a tumor uptake of 32.28 ± 6.95% ID g^{-1} at 1 h p.i., and 11.63 ± 1.24% ID g^{-1} at 24 h p.i. Compared to [^{111}In-DOTA0,Tyr3]octreotate, ^{111}In-labeled **16** showed a higher uptake in the pancreas, stomach and kidney at 1 h p.i. (15.77 ± 3.44, 19.27 ± 0.93, and 39.65 ± 6.20% ID g^{-1} respectively). Notably, due to fast wash-out from the tissue, the radioactivity in

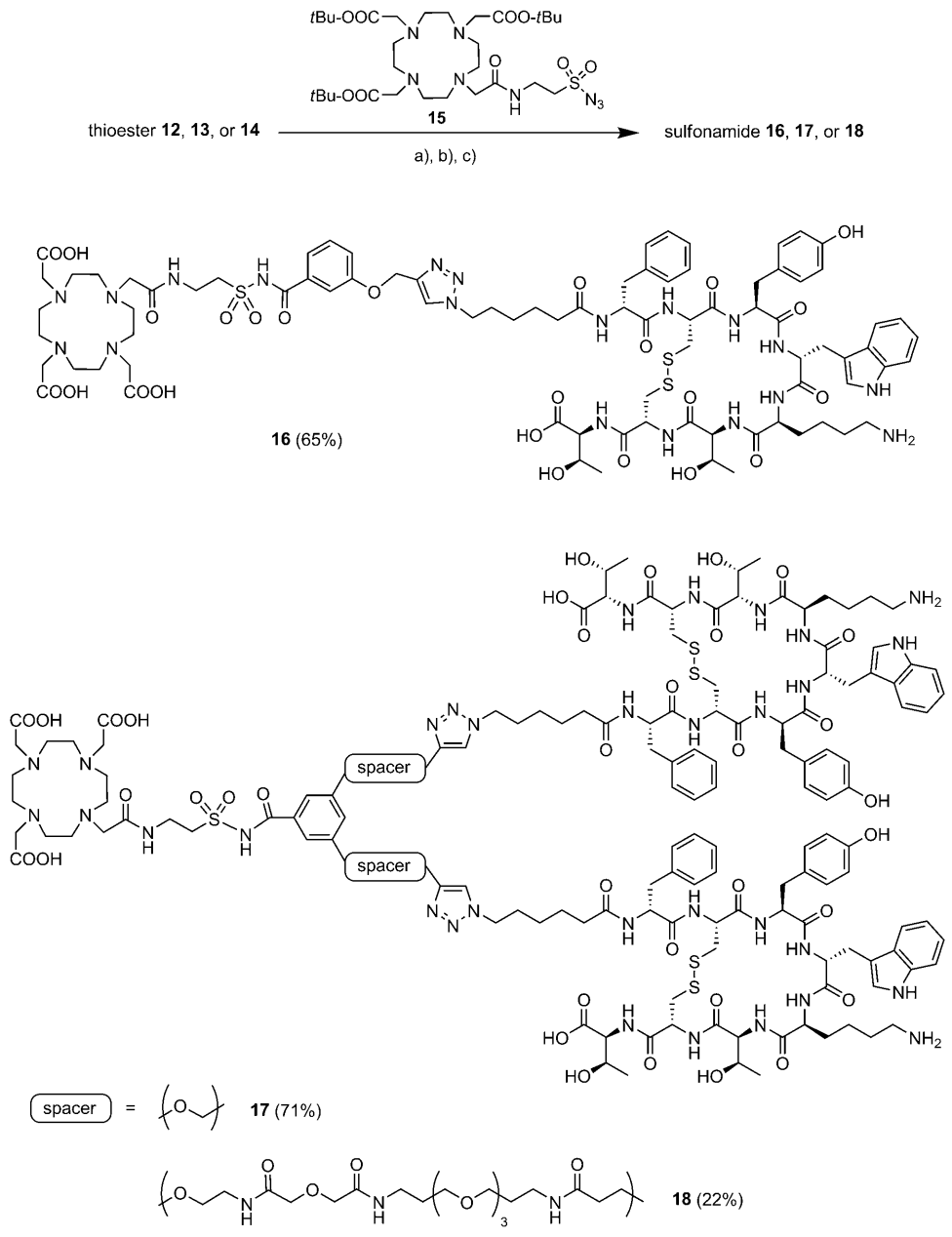

Scheme 6. Synthesis of mono- and dimeric DOTA-conjugated [Tyr3]octreotate sulfonamides **16**–**18** by the "sulfo-click" method. a) TFA/TiPS (95:5, *v/v*), 3 h, RT; b) **15**, 2,6-lutidine, DMF (4 Å molecular sieves), 1 h, RT; c) TFA/TiPS/H_2O (95:2.5:2.5, *v/v/v*), 3 h, RT.

pancreas, stomach, and kidney declined to 2.94 ± 0.60, 8.43 ± 1.13, and 13.09 ± 1.05 % ID g^{-1}, respectively, at 4 h p.i. Its blood clearance was fast (1.23 ± 0.27 % ID g^{-1} at 1 h p.i., 0.04 ± 0.01 % ID g^{-1} at 24 h p.i.) with the tumor/blood ratios increasing from 29.2 ± 25.2 at 1 h p.i. to 268 ± 204 at 24 h p.i. The incorporated synthetic core with both the sulfonamide and triazole linker did not influence tumor targeting, as was demonstrated by the similar values for tumor uptake of [^{111}In-DOTA0,Tyr3]octreotate and ^{111}In-labeled **16**.

^{111}In-labeled dimeric [Tyr3]octreotate **17**, which includes a nine-atom spacer, showed a high and specific tumor uptake of 38.80 ± 8.33 % ID g^{-1} at 1 h p.i. (Figure 4 B, Table 2). Interestingly, the activity in the tumor remained high at 4 h p.i. (40.87 ± 2.51 % ID g^{-1}); this indicates prolonged retention of this compound in the tumor. This enhanced retention can be explained by the increased receptor binding rate of ^{111}In-labeled dimer **17**, observed during in vitro experiment (Figure 3 A). At 24 h p.i., however, the accumulated radioactivity in tumor of ^{111}In-labeled **17** (13.45 ± 2.23 % ID g^{-1}) was similar to that of ^{111}In-labeled [Tyr3]octreotate monomer **16** (9.89 ± 1.20 % ID g^{-1}).

A number of studies have reported the effects of specific hydrophilic, acidic, or basic linkers on the in vivo characteristics, and it was found that these linkers are important in reducing radiotracer accumulation in nontumor tissue, and consequently increasing the tumor/background ratios.[6e,19] The introduction of the extended hydrophilic 57-atom spacer, as in the case of ^{111}In-labeled dimer **18**, led to rapid clearance from the blood pool, and decreased uptake in the lung, spleen, pancreas, stomach, and liver, when compared to [Tyr3]octreotate dimer **17** (Figure 4 C). Unfortunately, the rapid wash-out of ^{111}In-labeled **18** from the circulation also decreased the radioactivity in the tumor to half the value of that of ^{111}In-labeled **17**. Apart from the low tumor uptake (21.36 ± 4.87 % ID g^{-1} at 1 h p.i.), radiolabeled **18** had a very high kidney accumulation (97.22 ± 3.70 at 1 h and 80.21 ± 4.70 at 24 h p.i.).

The comparable tumor uptake at 1 h p.i. of [^{111}In-DOTA0,-Tyr3]octreotate, ^{111}In-labeled **16**, and ^{111}In-labeled **17** were in accordance with the IC_{50} values determined in vitro. The unfavorable tumor accumulation of ^{111}In-labeled **18** could be due to a combination of rapid wash-out from the circulation, high kidney accumulation, and a relatively lower internalization rate (Figure 3 B).

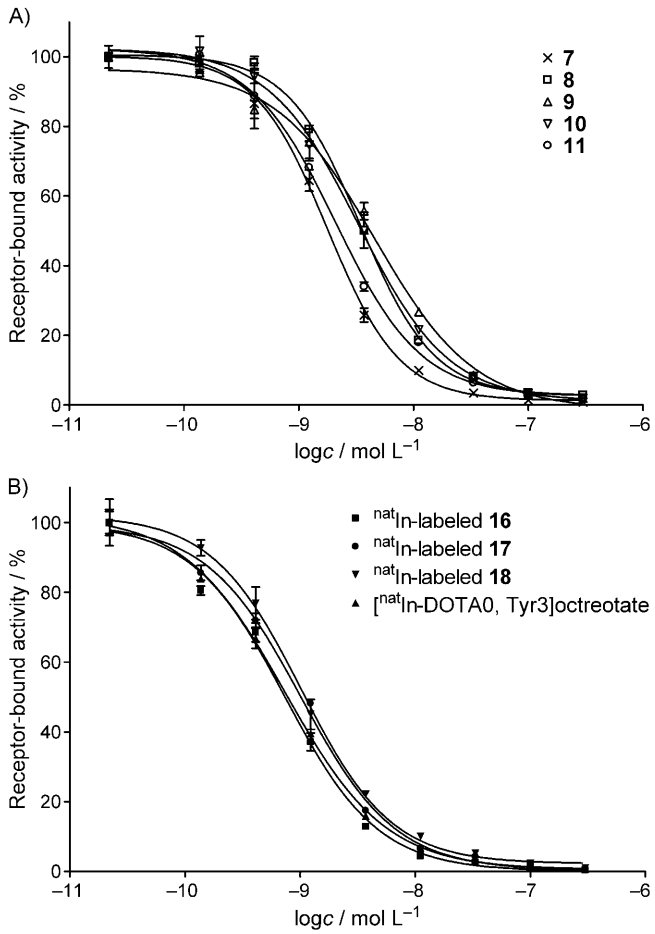

Figure 2. Displacement of [^{111}In-DOTA0,Tyr3]octreotate from binding sites on AR42J tumor cells by increasing concentration of non-radioactive competitor. A) Displacement by dimeric [Tyr3]octreotate conjugates **8**, **9**, **10**, and **11**. Monomeric [Tyr3]octreotate conjugate **7** was used as a reference. B) Displacement by mono- and dimeric ^{nat}In-DOTA-conjugated [Tyr3]octreotate **16**, **17**, and **18**. [^{nat}In-DOTA0,Tyr3]octreotate was used as a reference (IC_{50}: 0.7 nM). The error bars indicate the range of the 95% confidence interval ($n=2$ for each data point).

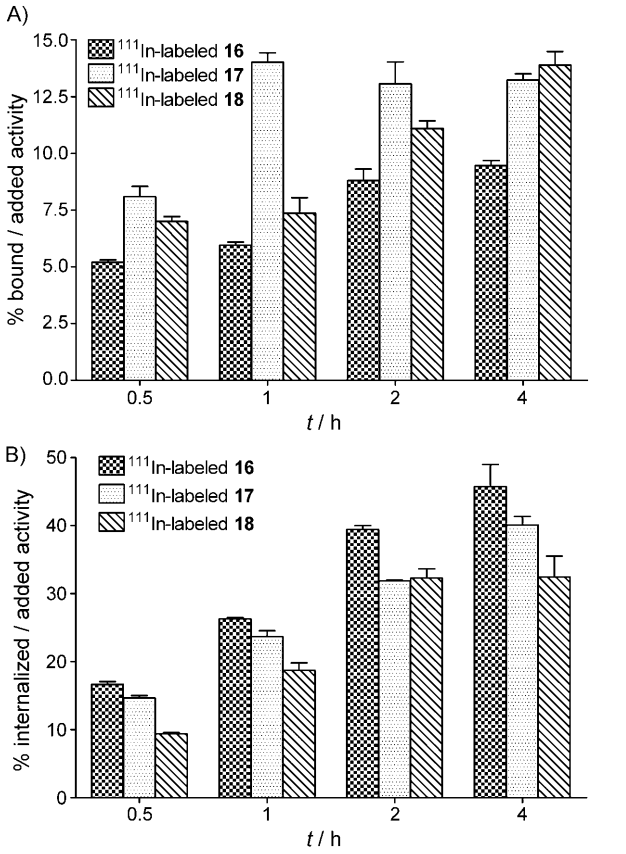

Figure 3. Time-dependent A) receptor binding and B) internalization of ^{111}In-labeled **16**–**18** by AR42J rat pancreatic tumor cells incubated for 30 min, 1, 2 and 4 h at 37 °C.

Conclusions

We have developed a versatile synthesis method, and have systemically investigated the binding properties of a series of dimeric [Tyr3]octreotate analogues, and evaluated the effects of different spacers between two cyclic [Tyr3]octreotate sequences on in vitro characteristics. From a competitive binding assay, the strongest dimeric binder—the [Tyr3]octreotate dimer with the longest spacer (57 atoms)—was selected for further DOTA-functionalization, radiolabeling, and in vivo evaluation. In addition, the DOTA-conjugated [Tyr3]octreotate dimer with the shortest spacer (nine atoms), and the corresponding monomeric DOTA-conjugated [Tyr3]octreotate analogue were included in the study to assess the effects of spacer length and dimerization, respectively, on tumor targeting and pharmacokinetic properties. These DOTA-conjugated mono- and dimeric [Tyr3]octreotate-based analogues were successfully prepared by using the two-stage click chemistry: Cu^{I}-catalyzed 1,3-dipolar "copper-click" cycloaddition followed by thio acid/sulfonylazide "sulfo-click" amidation. Biodistribution studies with ^{111}In-labeled compounds were evaluated in a BALB/c nude mouse model with subcutaneous inoculated AR42J pancreatic tumors. The ^{111}Inlabeled dimeric [Tyr3]octreotate analogue with a nine-atom spacer had a high tumor uptake (38.8 ± 8.3% ID g^{-1}) at 1 h p.i., which was maintained at 4 h p.i. (40.9 ± 2.5% ID g^{-1}). However, the introduction of the long hydrophilic 57-atom spacer into our dimeric [Tyr3]octreotate design resulted in higher kidney uptake and faster clearance from the circulation, with concomitantly lower tumor accumulation (21.36 ± 4.87% ID g^{-1} at 1 h p.i.). These findings provide important information about spacer length effects of dimeric [Tyr3]octreotate peptides on tumor targeting and pharmacokinetics. This can be translated into future research towards applications of [Tyr3]octreotate-based conjugates.

Experimental Section

Reagents, materials and analysis methods: Unless stated otherwise, chemicals were obtained from commercial sources and used without purification. Peptide-grade solvents were purchased from Biosolve (Valkenswaard, the Netherlands) and used directly, except for *N*,*N*-dimethylformamide (DMF), *N*-methylpyrrolidone (NMP), and dichloromethane (DCM), which were dried on 4 Å molecular sieves

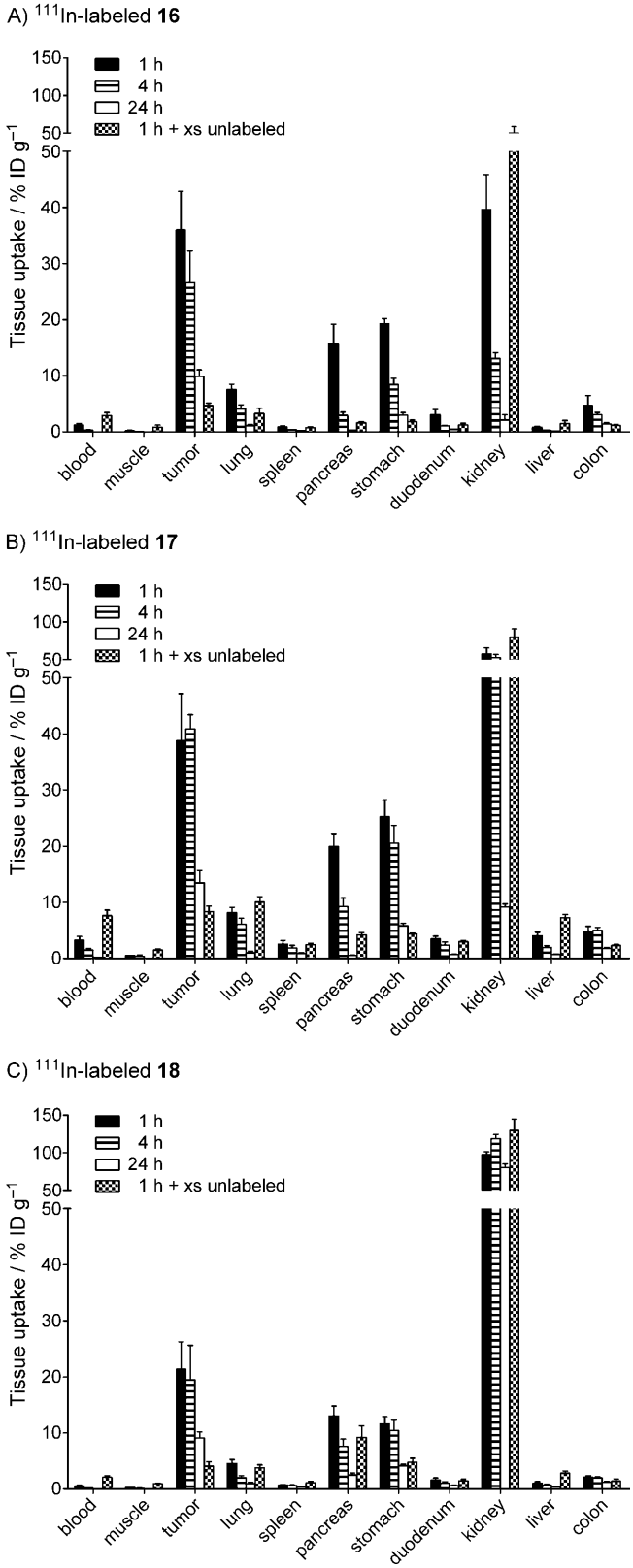

Figure 4. Biodistribution of A) ^{111}In-labeled [Tyr3]octreotate analogue **16**, B) [Tyr3]octreotate dimer **17** (nine-atom spacer), and C) [Tyr3]octreotate dimer **18** (57-atom spacer) in BALB/c nude mice bearing subcutaneous AR42J-expressing tumors in the right flank. Values are given as percentages of the injected dose per gram of tissue ($n=5$ mice/group). Blocking was performed by coinjection of octreotide. Mice were dissected at 1, 4, and 24 h p.i. ID: injected dose.

Table 2. Biodistribution of ^{111}In-labeled monomeric (**16**) and dimeric (**17** and **18**) [Tyr3]octreotate DOTA-conjugated analogues in AR42J tumor-bearing BALB/c nude mice at 1, 4, and 24 h p.i.[a]

	Time after injection			
	1 h	4 h	24 h	1 h + cold
^{111}In-labeled monomer **16**				
blood	1.23 ± 0.27	0.29 ± 0.10	0.04 ± 0.01	2.91 ± 0.55
tumor	35.99 ± 6.89	26.62 ± 5.62	9.89 ± 1.20	4.69 ± 0.43
pancreas	15.77 ± 3.44	2.94 ± 0.60	0.29 ± 0.02	1.62 ± 0.21
stomach	19.27 ± 0.93	8.43 ± 1.13	2.97 ± 0.49	1.82 ± 0.29
kidney	39.65 ± 6.20	13.09 ± 1.05	2.13 ± 0.94	50.06 ± 8.71
liver	0.83 ± 0.18	0.26 ± 0.03	0.11 ± 0.01	1.51 ± 0.53
^{111}In-labeled dimer **17**				
blood	3.24 ± 0.69	1.46 ± 0.31	0.16 ± 0.04	7.60 ± 1.00
tumor	38.80 ± 8.33	40.87 ± 2.51	13.45 ± 2.23	8.31 ± 1.02
pancreas	19.92 ± 2.19	9.24 ± 1.55	0.54 ± 0.05	4.19 ± 0.41
stomach	25.28 ± 2.92	20.52 ± 3.20	5.82 ± 0.43	4.36 ± 0.18
kidney	57.71 ± 7.90	52.34 ± 4.35	9.18 ± 0.55	79.7 ± 11.1
liver	4.03 ± 0.63	1.94 ± 0.30	0.72 ± 0.04	7.23 ± 0.64
^{111}In-labeled dimer **18**				
blood	0.58 ± 0.11	0.16 ± 0.17	0.03 ± 0.001	2.08 ± 0.27
tumor	21.36 ± 4.87	19.46 ± 6.14	9.09 ± 1.12	4.08 ± 0.77
pancreas	13.03 ± 1.75	7.58 ± 1.33	2.47 ± 0.36	9.20 ± 2.04
stomach	11.60 ± 1.30	10.42 ± 2.01	4.15 ± 0.26	4.77 ± 0.69
kidney	97.22 ± 3.70	118.5 ± 5.7	80.21 ± 4.70	129.6 ± 14.8
liver	1.06 ± 0.24	0.67 ± 0.16	0.38 ± 0.04	2.81 ± 0.39

[a] Each value represents the mean % injected dose per g of tissue ± SD of five animals. Mean tumor weight was 0.20 g.

prior to (solid-phase) synthesis. Tentagel S PHB resin was purchased from Rapp Polymere (Tübingen, Germany), and N^{α}-fluorenylmethyloxycarbonyl (Fmoc) amino acids were purchased from Advanced ChemTech, Alexis, or Novabiochem. [DOTA0,Tyr3]octreotate was purchased from Bachem (Bubendorf, Switzerland). Commercially available (Novartis) octreotide ("Sandostatin") was used as a receptor-selective ligand. Solid-phase synthesis was carried out in plastic syringes with polyethylene frits (20 μm) obtained from Applied Separations Inc. Resin loading was determined by measuring the UV absorbance of the piperidine–dibenzofulvene adduct ($\lambda_{max}=300$ nm).[20] Analytical thin-layer chromatography (TLC) and R_f values were determined on Merck precoated silica-gel 60 F-254 (0.25 mm) plates. Spots were visualized with UV light, ninhydrin, or Cl_2/*N*,*N*,*N*′,*N*′-tetramethyl-4,4′-diaminodiphenylmethane (TDM).[21] Column chromatography was performed on Silicycle silica-gel (60 Å, particle size 41–63 μm) by using distilled solvents. Microwave irradiation was performed in a Biotage Initiator (300 W). ^{1}H NMR spectra were recorded on a Varian G-300 spectrometer (300 MHz), and chemical shifts are given in ppm (δ) relative to TMS (0.00 ppm). ^{13}C NMR spectra were recorded on a Varian G-300 spectrometer (75.5 MHz), and chemical shifts are given in ppm (δ) relative to $CDCl_3$ (77.0 ppm). The ^{13}C NMR spectra were recorded by using the attached proton test (APT) sequence. Analytical reversed-phase HPLC was accomplished on a Shimadzu HPLC system, and (semi)-preparative reversed-phase HPLC was accomplished on a Kratos HPLC workstation. The mobile phase was 0.1% trifluoroacetic acid (TFA) in CH_3CN/H_2O (5:95, *v*/*v*; solvent A), and 0.1% TFA in CH_3CN/H_2O (95:5, *v*/*v*; solvent B). Analytical HPLC runs were performed on an Alltech Alltima C_8 column (250×4.6 mm, pore size 90 Å, particle size 5 μm) by using a linear gradient of solvent B (0–100% in 20 min) in solvent A at a flow rate of 1.0 mL min^{-1}. All preparative HPLC runs were performed on an Alltech Adsorbosphere XL C_8 column (250×22 mm, pore size 90 Å, particle size 10 μm, 12.0 mL min^{-1}), and semi-preparative HPLC

runs were performed on an Alltech Alltima C_8 column (250× 10 mm, pore size 90 Å, particle size 10 μm, 4.8 mL min^{-1}). The gradient consisted of 100% solvent A for 5 min, to 100% solvent B in 120 min. The purity of all newly synthesized compounds was judged by analytical HPLC and was found to be at least 98%. MALDI-ToF analysis was performed on a Kratos Axima CFR apparatus with human ACTH(18–39) (2465.2 $[M+H]^+$), or bovine insulin oxidized B chain (3494.7 $[M+H]^+$) as the external reference, and α-cyano-4-hydroxycinnamic acid as matrix. High-resolution electrospray ionization (ESI) mass spectra were measured on a Micromass LCT mass spectrometer calibrated with CsI by using nano-ESI at 1200 V capillary voltage and 50 V at the sample cone. All reported mass values are monoisotopic.

Chemistry: The syntheses of dihydroxybenzoic acid-based alkynes **2a**–**6a** have been described previously.[18] The syntheses of **2b**, **3b**, and **15** have been reported earlier by Yim et al.[12] Details of the synthesis and characterization of **7**–**11**, **13**, and **14** are described in the Supporting Information.

*Ahx-D-Phe-cyclo(Cys-Tyr-D-Trp-Lys-Thr-Cys)-Thr-OH (**1**)*: All reagents and glassware were dried in vacuo for 18 h before use. Wang resin (3.7 g (1.0 mmol), 0.27 mmol g^{-1}) was swollen (DCM) and washed (DMF) prior to loading of the first amino acid. Fmoc-Thr(*t*Bu)-OH (2.0 g, 5 mmol) was dissolved in DMF (5 mL), dried on 4 Å molecular sieves, and added to the resin, followed by pyridine (0.7 mL, 8 mmol). The obtained slurry was gently swirled for 30 min until the amino acid derivative dissolved completely. Then, 2,6-dichlorobenzoyl chloride (DCBC: 0.7 mL, 5 mmol) was added, and the mixture was gently swirled for 18 h at room temperature. The resin was subsequently washed (DMF, DCM) and dried. The resin loading was 68% (0.18 mmol g^{-1}), as calculated from an Fmoc determination. The linear peptide sequence was synthesized according to Fmoc/*t*Bu solid phase peptide synthesis protocols. After coupling of N-terminal 6-azido-hexanoic acid, the resin was washed (NMP, DCM), dried, and suspended in TFA/H_2O/*Ti*PS (20 mL, 95:2.5:2.5, *v*/*v*/*v*), and stirred for 3 h to cleave the peptide from the resin, and to remove the side chain protecting groups. The crude peptide was isolated by precipitation (3×) with cold (−20 °C) MTBE/hexane (1:1, *v*/*v*). After centrifugation, the pellet was dissolved in acetonitrile/water (1:1, *v*/*v*), lyophilized, and purified by HPLC. This linear peptide (45 mg, 38 μmol) was subsequently dissolved in acetonitrile/water (1:1, *v*/*v*), and DMSO (10%) was added to this solution. The pH was adjusted to 7.5 with 5% aqueous ammonia. After stirring overnight at room temperature, the solution was partially concentrated in vacuo, and the remaining DMSO was evaporated with a rotational vacuum concentrator (Christ, Alpha-RVC). Following preparative HPLC, the cyclic peptide was obtained in an overall yield of 24% (36 mg). R_t: 20.07 min (C_8); ESI-MS: *m*/*z* 1188.35 $[M+H]^+$, 1210.40 $[M+Na]^+$; calcd for $C_{55}H_{73}N_{13}O_{13}S_2$: 1187.49.

S-2,4,6-Trimethoxybenzyl 3,5-bis((4,8,24-trioxo-6,13,16,19-tetraoxa-3,9,23-triazaoctacos-27-yn-1-yl)oxy)benzothioate (**6b**): Ethyl-3-(3-dimethylaminopropyl)carbodiimide (EDCI, 47 mg, 0.245 mmol), 2,4,6-trimethoxybenzylthiol (35 mg, 0.163 mmol) and a catalytic amount of 4-dimethylaminopyridine (DMAP, 2 mg, 0.002 mmol) were added to a solution of **6a** (170 mg, 0.163 mmol) in dry DMF (10 mL). The yellowish solution was stirred overnight under nitrogen atmosphere at room temperature. After evaporating the solvent, the product was isolated by silica column chromatography by using a gradient of DCM/MeOH (95:5 to 90:10, *v*/*v*). The 2,4,6-trimethoxybenzyl-protected dialkyne was obtained as a colorless oil in 58% yield (117 mg, 94.9 μmol). R_f = 0.40 (methanol/dichloromethane, 1:9); ^{1}H NMR (CD_3OD): δ = 1.74–1.83 (m, 8H; 4$CH_2CH_2CH_2$), 2.30 (t, J = 2.6 Hz, 2H; 2CCH), 2.39 (m, 4H; 2CHCCH_2), 2.47 (m, 4H; 2C(O)C$H_2$$CH_2$), 3.25–3.48 (m, 8H; 2OC$H_2$$CH_2$NH, 2$CH_2CH_2$C(O)C$H_2$), 3.50–3.70 (m, 28H; 12$OCH_2$, 2OC$H_2$C(O)NHC$H_2$), 3.83–3.84 (m, 9H; 3$OCH_3$), 4.05 (s, 4H; 2C(O)C$H_2$O), 4.10 (s, 4H; 2C(O)C$H_2$O), 4.14 (t, J = 5.4 Hz, 4H; 2OCH_2CH_2NH), 4.34 (s, 2H; SCH_2), 6.23 (s, 2H; 2CH_3OCCH), 6.79 (t, J = 2.2 Hz, 1H; CH_2OCC*H*), 7.09 (d, J = 2.5 Hz, 2H; 2C(O)CC*H*); ^{13}C NMR ($CDCl_3$): δ = 15.8 (CH_2CCH), 23.6 (SCH_2), 30.4 ($CH_2CH_2CH_2$), 36.1 (C(O)CH_2CH_2), 37.7 and 37.8 (C(O)NH$CH_2CH_2CH_2$), 39.6 (OCH_2CH_2NH), 55.9 and 56.4 (OCH_3), 67.9 (OCH_2CH_2NH), 69.8 and 70.0 (C(O)CH_2O), 70.4 (CH_2CCH), 71.2 and 71.5 (OCH_2), 83.7 (CH_2CCH), 91.6 (CH_3OCCH), 105.2 (SCH_2C), 106.7 (CH_2OCCH), 107.3 (SC(O)CCH), 140.7 (SC(O)*C*), 160.6 (CH_3OC), 161.4 (CH_2OC), 162.8 (CH_3OC), 171.5, 172.0 and 174.0 (C(O)NH), 193.9 (*SC*(O)).

*Monomeric [Tyr3]octreotate peptide thio ester (**12**)*: Aqueous $CuSO_4$ (47 μL, 4.8 μmol) and Na ascorbate (47 μL, 23 μmol) were added to a solution of azide **1** (10.8 mg, 9.1 μmol) and alkyne **2b** (3.5 mg, 9.5 μmol) in THF/H_2O (3:1, *v*/*v*, 0.3 mL). The reaction mixture was stirred for 16 h at room temperature. Then, the solvents were removed under reduced pressure and the residue was taken up in CH_3CN/H_2O and purified by semipreparative HPLC (C_4). Compound **12** was obtained in 66% yield (6.0 μmol, 9.4 mg). R_t(C_4): 32.5 min. ESI-MS: *m*/*z* 1560.8 $[M+H]^+$, 1582.8 $[M+Na]^+$, 780.9 $[M+2H]^{2+}$; calcd for $C_{75}H_{93}N_{13}O_{18}S_3$: 1559.59.

*DOTA-conjugated monomeric [Tyr3]octreotate sulfonamide (**16**)*: Peptide thio ester **12** (3.7 mg, 2.3 μmol) was treated with TFA/*Ti*PS (95:5, *v*/*v*; 400 μL) for 3 h at room temperature. After concentration in vacuo, the residue was dissolved in dry DMF (120 μL), then sulfonyl azide **15** (1.7 mg, 2.4 μmol) followed by 2,6-lutidine (2.0 μL, 17 μmol) were added. The reaction mixture was stirred for 1 h at room temperature and subsequently concentrated in vacuo. This residue was treated with TFA/*Ti*PS/H_2O (95:2.5:2.5, *v*/*v*/*v*) for 3 h at room temperature. Compound **16** was obtained in 65% yield (2.8 mg, 1.51 μmol) after purification by semipreparative HPLC. R_t(C_8): 18.28 min; ESI-MS: *m*/*z* 1857.0 $[M+H]^+$, 929.0 $[M+2H]^{2+}$, 619.6 $[M+3H]^{3+}$; calcd for $C_{83}H_{113}N_{19}O_{24}S_3$: 1855.74.

*DOTA-conjugated dimeric [Tyr3]octreotate C_9-spacer sulfonamide (**17**)*: The synthesis of **17** was performed as described for **16**, but starting from thio ester **13** (1.7 mg, 0.6 μmol) and sulfonyl azide **15** (0.9 mg, 1.3 μmol). Compound **17** was obtained in 71% yield (1.3 mg, 0.42 μmol) after purification. R_t(C_8): 18.82 min; ESI-MS: *m*/*z* 1549.7 $[M+2H]^{2+}$, 1033.5 $[M+3H]^{3+}$, 775.4 $[M+4H]^{4+}$; calcd for $C_{141}H_{188}N_{32}O_{38}S_5$: 3097.24.

*DOTA-conjugated dimeric [Tyr3]octreotate C_{57}-spacer sulfonamide (**18**)*: The same procedure as described for **16** was used, but starting from thio ester **14** (8.4 mg, 2.3 μmol) and sulfonyl azide **15** (1.7 mg, 2.4 μmol). Compound **18** was isolated after column chromatography in 22% yield (2.0 mg, 0.51 μmol). R_t(C_8): 18.50 min; ESI-MS: *m*/*z* 1953.0 $[M+2H]^{2+}$, 1302.3 $[M+3H]^{3+}$, 977.0 $[M+4H]^{4+}$, 781.8 $[M+5H]^{5+}$; calcd for $C_{177}H_{254}N_{38}O_{52}S_5$: 3903.70.

Cell line and culture conditions: The AR42J cell-line was kindly provided by the Erasmus Medical Center (Rotterdam, The Netherlands). These cells were cultured in Dulbecco's modified Eagle's medium (DMEM, Gibco) supplemented with 10% fetal calf serum, 1% penicillin/streptomycin and 1% glutamine. The cultures were maintained in a humidified atmosphere (5% CO_2/95% air, 37 °C) and routinely passed by using a trypsin-ethylenediaminetetraacetic acid solution (Invitrogen).

Receptor binding studies: The half-maximal inhibitory concentration (IC_{50}) of the peptides for binding to SSTR2 was determined on AR42J tumor cells in a competitive binding assay with [^{111}In-DO-

TA0,Tyr3]octreotate as a tracer. AR42J cells were seeded into six-well plates at 8×10^5 cells/well and cultured until confluent. Cells were washed twice with binding buffer (DMEM with 0.1% *w/v* bovine serum albumin). Subsequently, binding buffer (1.5 mL), non-radioactive competitor (from 0.1 to 300 nM), and a trace amount of radiotracer (100 Bq) were added to each well. After incubation (37 °C for 3 h), the medium was removed, and cells were washed twice with binding buffer, extracted from the wells, and cell-associated radioactivity was determined in a γ-counter. For the "cold" labeling of **16**–**18** with $^{nat}In^{3+}$, each of the peptides was dissolved in an aqueous solution (25 μL, 10 mM NH_4OAc). Subsequently, a three molar excess of $InCl_3$ (Aldrich) was added. The In^{III} complexation was performed at 95 °C for 15 min. GraphPad Prism software (version 4.00 for Windows, GraphPad Software) was used to calculate IC_{50} values and to determine statistical significance at the 95% confidence interval, with $P<0.05$ being considered significantly different.

Radiolabeling: DOTA-conjugated peptides were labeled with $^{111}InCl_3$ (Covidien) in 2-(*N*-morpholino)ethanesulfonic acid (MES) solution (0.1 M, pH 5.5) for 15 min at 95 °C. Labeling reactions were performed in acid-washed Protein LoBind safe-lock tubes (Eppendorf GmbH). Radiochemical purity was determined by instant thin-layer chromatography (ITLC) on silica gel (Tec-Control Chromatography Strips, Biodex Medical Systems, Inc). The ITLC analysis was performed by using two different mobile phases: 0.1 M ethylenediaminetetraacetic acid (EDTA)/0.1 M NH_4OAc (1:1, *v/v*) (R_f bound $^{111}In=0$, R_f unbound $^{111}In=1$) and THF/0.25 M NH_4OAc (1:1, *v/v*; R_f colloid = 0, R_f unbound ^{111}In or ^{111}In-labeled compound >0.5).

Octanol–saline partition coefficient: ^{111}In-labeled **16**, **17**, or **18** (ca. 370 kBq, ~10 μL) was added to a mixture of saline (500 μL, pH 7.4) and *n*-octanol (500 μL). The resulting biphasic system was shaken vigorously for 2 min, and the two layers were subsequently separated by centrifugation (5 min, 250 *g*). The radioactivity levels in 100 μL aliquots ($n=3$) of both the organic and the aqueous layers were measured in a γ-counter (Perkin–Elmer). The partition coefficient ($\log D$) was determined from at least two independent experiments, and calculated from the formula $\log D=\log_{10}$ (counts in octanol layer/counts in aqueous layer).

In vitro stability in serum: ^{111}In-labeled **16**, **17**, or **18** (~370 kBq, ~10 μL) was incubated with human serum (300 μL) at 37 °C for up to three days. Following incubation at selected time points, the serum proteins were precipitated with acetonitrile (1:1, *v/v*), and the sample was centrifuged (5 min, 5000 *g*). The supernatant layer was filtered and analyzed on an Agilent HPLC system with an in-line NaI radiodetector (Raytest GmbH) by using an Alltech Alltima C_{18} column (250×4.6 mm, pore size: 100 Å, particle size: 5 μm, 1.0 mL min^{-1}) with a linear gradient of buffer B (5–100% over 20 min) in buffer A. (Buffer A: 0.1% TFA in water; buffer B: 0.1% TFA in acetonitrile.)

Internalization: Internalization of ^{111}In-labeled **16**–**18** by AR42J cells was studied as described earlier.[22] Cells were grown to confluency in six-well plates, and were incubated with trace amounts (ca. 0.1 nM) of radiolabeled peptide for 30 min, 1, 2, and 4 h at 37 °C. Cell surface-bound radioligand was removed by washing the cells with cold acidic buffer (0.1 M acetic acid, 154 mM NaCl, pH 2.6). Internalized radioligand was determined as the cell-associated radioactivity which was not removed by this procedure. The experiment was performed in triplicate, and nonspecific binding was determined from a parallel series containing 0.4 μM octreotide ("Sandostatin").

Biodistribution: All animal experiments were conducted in compliance with the animal welfare committee requirements of our institution, and performed according to national regulations. Six- to seven-week-old male BALB/c nude mice were inoculated subcutaneously with AR42J cells (10^7) in the right flank. Mice received irradiated chow and acidified drinking water ad libitum. After eleven days, when tumors had an average mass of 0.2 g, mice were randomly divided into groups of five. Each group received intravenous injections of 0.37 MBq (0.1 μg) ^{111}In-labeled peptides **16**, **17**, or **18** into the tail vein. At 1, 4, or 24 h p.i. the animals were euthanized by CO_2/O_2 asphyxiation. Blood, tumor and tissues of interest were dissected, weighed and counted in a γ-counter along with three aliquots (100 μL) of the diluted standard (representing 1% of the injected activity). From this, the percentage injected dose per gram (% ID g^{-1}) for each tissue was calculated. Additional groups of five mice were coinjected intravenously with 50 μg octreotide and euthanized after 1 h to determine nonspecific binding of the radiotracers.

Acknowledgements

The authors thank Prof. Marion de Jong for providing the rat pancreatic AR42J tumor cell-line. Bianca Lemmers, Kitty Lemmens, Gerben Franssen, Sandra Heskamp, and Cathelijne Frielink are gratefully acknowledged for biotechnical assistance during in vivo experiments, and Hans Jacobs is thanked for technical support and scientific discussions during the synthesis of dimeric [Tyr3]octreotate peptides. Hans Hilbers is thanked for MALDI-ToF measurements.

Keywords: click chemistry · dimerization · radiopharmaceuticals · receptor binding · somatostatin receptors

[1] a) P. Brazeau, W. Vale, R. Burgus, N. Ling, M. Butcher, J. Rivier, R. Guillemin, *Science* **1973**, *179*, 77–79; b) R. Guillemin, J. E. Gerich, *Annu. Rev. Med.* **1976**, *27*, 379–388; c) S. Reichlin, *N. Engl. J. Med.* **1983**, *309*, 1495–1501; d) S. Reichlin, *N. Engl. J. Med.* **1983**, *309*, 1556–1563; e) J. Epelbaum, *Prog. Neurobiol.* **1986**, *27*, 63–100.

[2] a) T. Reisine, *Am. J. Physiol.* **1995**, *269*, G813-G820; b) Y. C. Patel, M. T. Greenwood, R. Panetta, L. Demchyshyn, H. Niznik, C. B. Srikant, *Life Sci.* **1995**, *57*, 1249–1265; c) G. Olias, C. Viollet, H. Kusserow, J. Epelbaum, W. Meyerhof, *J. Neurochem.* **2004**, *89*, 1057–1091; d) U. Kumar, M. Grant, *Results Probl. Cell Differ.* **2010**, *50*, 137–184.

[3] a) D. F. Veber, R. M. Freidlinger, D. S. Perlow, W. J. Paleveda, Jr., F. W. Holly, R. G. Strachan, R. F. Nutt, B. H. Arison, C. Homnick, W. C. Randall, M. S. Glitzer, R. Saperstein, R. Hirschmann, *Nature* **1981**, *292*, 55–58; b) W. Bauer, U. Briner, W. Doepfner, R. Haller, R. Huguenin, P. Marbach, T. J. Petcher, J. Pless, *Life Sci.* **1982**, *31*, 1133–1140; c) W. A. Murphy, V. A. Lance, S. Moreau, J. P. Moreau, D. H. Coy, *Life Sci.* **1987**, *40*, 2515–2522; d) M. de Jong, W. A. P. Breeman, W. H. Bakker, P. P. M. Kooij, B. F. Bernard, L. J. Hofland, T. J. Visser, A. Srinivasan, M. A. Schmidt, J. L. Erion, J. E. Bugaj, H. R. Mäcke, E. P. Krenning, *Cancer Res.* **1998**, *58*, 437–441; e) I. Virgolini, M. Leimer, H. Handmaker, S. Lastoria, C. Bischof, P. Muto, T. Pangerl, D. Gludovacz, M. Peck-Radosavljevic, J. Lister-James, G. Hamilton, K. Kaserer, P. Valent, R. Dean, *Cancer Res.* **1998**, *58*, 1850–1859; f) W. G. Rajeswaran, S. J. Hocart, W. A. Murphy, J. E. Taylor, D. H. Coy, *J. Med. Chem.* **2001**, *44*, 1416–1421; g) J. E. Rivier, C. Hoeger, J. Erchegyi, J. Gulyas, R. DeBoard, A. G. Craig, S. C. Koerber, S. Wenger, B. Waser, J.-C. Schaer, J. C. Reubi, *J. Med. Chem.* **2001**, *44*, 2238–2246; h) J. C. Reubi, K.-P. Eisenwiener, H. Rink, B. Waser, H. R. Mäcke, *Eur. J. Pharmacol.* **2002**, *456*, 45–49; i) C. Bruns, I. Lewis, U. Briner, G. Meno-Tetang, G. Weckbecker, *Eur. J. Endocrinol.* **2002**, *146*, 707–716; j) A. M. Crider, *Mini Rev. Med. Chem.* **2002**, *2*, 507–517; k) G. Weckbecker, I. Lewis, R. Albert, H. A.

Schmid, D. Hoyer, C. Bruns, *Nat. Rev. Drug Discovery* **2003**, *2*, 999 – 1017; l) A. Di Cianni, A. Carotenuto, D. Brancaccio, E. Novellino, J. C. Reubi, K. Beetschen, A. M. Papini, M. Ginanneschi, *J. Med. Chem.* **2010**, *53*, 6188 – 6197.

[4] a) D. J. Kwekkeboom, J. Mueller-Brand, G. Paganelli, L. B. Anthony, S. Pauwels, L. K. Kvols, T. M. O'Dorisio, R. Valkema, L. Bodei, M. Chinol, H. R. Mäcke, E. P. Krenning, *J. Nucl. Med.* **2005**, *46*, 62S – 66S; b) F. Forrer, R. Valkema, D. J. Kwekkeboom, M. de Jong, E. P. Krenning, *Best Pract. Res. Clin. Endocrinol. Metab.* **2007**, *21*, 111 – 129; c) M. de Jong, W. A. P. Breeman, D. J. Kwekkeboom, R. Valkema, E. P. Krenning, *Acc. Chem. Res.* **2009**, *42*, 873 – 880; d) D. J. Kwekkeboom, B. L. Kam, M. van Essen, J. J. M. Teunissen, C. H. J. van Eijck, R. Valkema, M. de Jong, W. W. de Herder, E. P. Krenning, *Endocr.-Relat. Cancer* **2010**, *17*, R53-R73.

[5] a) A. Varki, *Glycobiology* **1993**, *3*, 97 – 130; b) M. Mammen, S.-K. Choi, G. M. Whitesides, *Angew. Chem.* **1998**, *110*, 2908 – 2953; *Angew. Chem. Int. Ed.* **1998**, *37*, 2754 – 2794; c) R. H. Kramer, J. W. Karpen, *Nature* **1998**, *395*, 710 – 713; d) P. I. Kitov, J. M. Sadowska, G. Mulvey, G. D. Armstrong, H. Ling, N. S. Pannu, R. J. Read, D. R. Bundle, *Nature* **2000**, *403*, 669 – 672; e) I. Vrasidas, S. André, P. Valentini, C. Böck, M. Lensch, H. Kaltner, R. M. J. Liskamp, H.-J. Gabius, R. J. Pieters, *Org. Biomol. Chem.* **2003**, *1*, 803 – 810; f) Z. Liu, J. Zhang, A. Zhang, *Curr. Pharm. Des.* **2009**, *15*, 682 – 718; g) Y. M. Chabre, R. Roy, *Adv. Carbohydr. Chem. Biochem.* **2010**, *63*, 165 – 393; h) S. G. Gouin, J. M. García Fernández, E. Vanquelef, F. Y. Dupradeau, E. Salomonsson, H. Leffler, M. Ortega-Muñoz, U. J. Nilsson, J. Kovensky, *ChemBioChem* **2010**, *11*, 1430 – 1442.

[6] a) M. Janssen, W. J. G. Oyen, L. F. A. G. Massuger, C. Frielink, I. Dijkgraaf, D. S. Edwards, M. Radjopadhye, F. H. M. Corstens, O. C. Boerman, *Cancer Biother. Radiopharm.* **2002**, *17*, 641 – 646; b) M. L. Janssen, W. J. Oyen, I. Dijkgraaf, L. F. Massuger, C. Frielink, D. S. Edwards, M. Rajopadhye, H. Boonstra, F. H. Corstens, O. C. Boerman, *Cancer Res.* **2002**, *62*, 6146 – 6151; c) I. Dijkgraaf, J. A. W. Kruijtzer, S. Liu, A. C. Soede, W. J. G. Oyen, F. H. M. Corstens, R. M. J. Liskamp, O. C. Boerman, *Eur. J. Nucl. Med. Mol. Imaging* **2007**, *34*, 267 – 273; d) Z. B. Li, K. Chen, X. Chen, *Eur. J. Nucl. Med. Mol. Imaging* **2008**, *35*, 1100 – 1108; e) I. Dijkgraaf, A. Y. Rijnders, A. Soede, A. C. Dechesne, G. W. Van Esse, A. J. Brouwer, F. H. M. Corstens, O. C. Boerman, D. T. S. Rijkers, R. M. J. Liskamp, *Org. Biomol. Chem.* **2007**, *5*, 935 – 944; f) S. Liu, *Bioconjugate Chem.* **2009**, *20*, 2199 – 2213.

[7] a) J. Shi, L. Wang, Y. S. Kim, S. Zhai, Z. Liu, X. Chen, S. Liu, *J. Med. Chem.* **2008**, *51*, 7980 – 7990; b) L. Wang, J. Shi, Y.-S. Kim, S. Zhai, B. Jia, H. Zhao, Z. Liu, F. Wang, X. Chen, S. Liu, *Mol. Pharm.* **2009**, *6*, 231 – 245; c) Z. Liu, G. Niu, J. Shi, S. L. Liu, F. Wang, S. Liu, X. Chen, *Eur. J. Nucl. Med. Mol. Imaging* **2009**, *36*, 947 – 957.

[8] a) M. Rocheville, D. C. Lange, U. Kumar, S. C. Patel, R. C. Patel, Y. C. Patel, *Science* **2000**, *288*, 154 – 157; b) M. Rocheville, D. C. Lange, U. Kumar, R. Sasi, R. C. Patel, Y. C. Patel, *J. Biol. Chem.* **2000**, *275*, 7862 – 7869; c) M. Grant, B. Collier, U. Kumar, *J. Biol. Chem.* **2004**, *279*, 36179 – 36183; d) M. Grant, U. Kumar, *Regul. Pept.* **2010**, *159*, 3 – 8.

[9] a) C. W. Tornøe, C. Christensen, M. Meldal, *J. Org. Chem.* **2002**, *67*, 3057 – 3064; b) V. V. Rostovtsev, L. G. Green, V. V. Fokin, K. B. Sharpless, *Angew. Chem.* **2002**, *114*, 2708 – 2711; *Angew. Chem. Int. Ed.* **2002**, *41*, 2596 – 2599.

[10] a) N. Shangguan, S. Katukojvala, R. Greenberg, L. J. Williams, *J. Am. Chem. Soc.* **2003**, *125*, 7754 – 7755; b) R. V. Kolakowski, N. Shangguan, R. R. Sauers, L. J. Williams, *J. Am. Chem. Soc.* **2006**, *128*, 5695 – 5702.

[11] a) R. Merkx, A. J. Brouwer, D. T. S. Rijkers, R. M. J. Liskamp, *Org. Lett.* **2005**, *7*, 1125 – 1128; b) D. T. S. Rijkers, R. Merkx, C.-B. Yim, A. J. Brouwer, R. M. J. Liskamp, *J. Pept. Sci.* **2010**, *16*, 1 – 5.

[12] C.-B. Yim, I. Dijkgraaf, R. Merkx, C. Versluis, A. Eek, G. E. Mulder, D. T. S. Rijkers, O. C. Boerman, R. M. J. Liskamp, *J. Med. Chem.* **2010**, *53*, 3944 – 3953.

[13] P. Sieber, *Tetrahedron Lett.* **1987**, *28*, 6147 – 6150.

[14] G. B. Fields, R. L. Noble, *Int. J. Pept. Protein Res.* **1990**, *35*, 161 – 214.

[15] J. P. Tam, C. R. Wu, W. Liu, J. W. Zhang, *J. Am. Chem. Soc.* **1991**, *113*, 6657 – 6662.

[16] D. T. S. Rijkers, G. W. van Esse, R. Merkx, A. J. Brouwer, H. J. F. Jacobs, R. J. Pieters, R. M. J. Liskamp, *Chem. Commun.* **2005**, 4581 – 4583.

[17] A. J. Brouwer, S. J. E. Mulders, R. M. J. Liskamp, *Eur. J. Org. Chem.* **2001**, 1903 – 1915.

[18] a) R. Autar, A. S. Khan, M. Schad, J. Hacker, R. M. J. Liskamp, R. J. Pieters, *ChemBioChem* **2003**, *4*, 1317 – 1325; b) A. V. Pukin, H. M. Branderhorst, C. Sisu, C. A. G. M. Weijers, M. Gilbert, R. M. J. Liskamp, G. M. Visser, H. Zuilhof, R. J. Pieters, *ChemBioChem* **2007**, *8*, 1500 – 1503; c) H. M. Branderhorst, R. M. J. Liskamp, G. M. Visser, R. J. Pieters, *Chem. Commun.* **2007**, 5043 – 5045.

[19] a) S. Liu, Z. J. He, W.-Y. Hsieh, Y.-S. Kim, Y. Jiang, *Bioconjugate Chem.* **2006**, *17*, 1499 – 1507; b) I. Dijkgraaf, S. Liu, J. A. W. Kruijtzer, A. C. Soede, W. J. G. Oyen, R. M. J. Liskamp, F. H. M. Corstens, O. C. Boerman, *Nucl. Med. Biol.* **2007**, *34*, 29 – 35; c) B. Jia, Z. Liu, J. Shi, Z. Yu, Z. Yang, H. Y. Zhao, Z. He, S. Liu, F. Wang, *Bioconjugate Chem.* **2008**, *19*, 201 – 210.

[20] J. Meienhofer, M. Waki, E. P. Heimer, T. J. Lambros, R. C. Makofske, C.-D. Chang, *Int. J. Pept. Protein Res.* **1979**, *13*, 35 – 42.

[21] E. von Arx, M. Faupel, M. Brugger, *J. Chromatogr.* **1976**, *120*, 224 – 228.

[22] L. J. Hofland, P. M. van Koetsveld, M. Waaijers, J. Zuyderwijk, W. A. Breeman, S. W. Lamberts, *Endocrinology* **1995**, *136*, 3698 – 3706.

Received: October 22, 2010
Published online on February 15, 2011

